


Article

Magnetic Anomaly and Model of the Lonar Meteorite Impact Crater in Maharashtra, India

Kalle Kiik ^{1,*} , Jüri Plado ¹, Muddaramaiah Lingadevaru ², Syed Hamim Jeelani ³
and Mateusz Szyszka ⁴

¹ Department of Geology, University of Tartu, Ravila 14A, Tartu 50411, Estonia; juri.plado@ut.ee

² Department of Geology, School of Earth Sciences, Central University of Karnataka,
Kalaburagi-585 367, Karnataka, India; mlingadevaru@cuk.ac.in

³ Department of Civil Engineering, Koneru Lakshmaiah Education Foundation. Deemed to be University,
Vaddeswaram-522502, Andhra Pradesh, India; hamim.syed@gmail.com

⁴ Department of Geology, Adam Mickiewicz University in Poznan, Krygowskiego 12, 61-680 Poznan, Poland;
Tauri01@gmail.com

* Correspondence: kalle.kiik2@gmail.com; Tel.: +372-581-49-866

Received: 10 September 2020; Accepted: 18 October 2020; Published: 20 October 2020



Abstract: The ground magnetic field of the Lonar impact crater (Maharashtra State, India) and its surrounding area was measured and studied utilizing 2.5-dimensional potential field modelling. Field data showed the crater depression is associated with a strong circular negative anomaly with an amplitude of more than 1000 nT. The negative anomaly, however, decreases smoothly while moving from south to north. Most of the crater rim exhibits anomalous positive values. Negative anomalies at the rim are seen in the south–southwestern sections and coinciding in the northeastern section with the Dhar valley. Our study shows that most of the anomaly is caused by the topographic effect and a strong SE directed natural remanent magnetization of Deccan Trap basalts, which are the target of the Lonar-creating projectile. The magnetic anomaly of the relatively weakly magnetized impact-produced allochthonous breccia and post-impact sediments is small, being less than 150 nT.

Keywords: magnetic anomaly; potential field modelling; Lonar; meteorite impact; applied geophysics; impact craters and processes

1. Introduction

The circular Lonar structure (19°58' N, 76°31' E) is located in Maharashtra State, Buldana District, India (Figure 1). It is a Quaternary-aged [1–3], 1.88 km diameter (D), simple meteorite impact crater formed into Deccan Trap basalts [4]. Thoughts of an impact origin can be attributed to [5], who mentioned the similarity of Lonar to Canyon Diablo (presently Barringer) Crater (although referring to their cryptovolcanic origin). Ref. [6] believed volcanic hypotheses were improbable, referring to the fact that no recent volcanism in India exists. A shallow bore-hole into the crater depression was drilled by [7] in 1961, providing information about the presence of crushed rock. Based on that drill-hole data and crater morphology, [8] noted several inconsistencies (absence of pyroclastics, young age, and the scale of the feature is too large for a steam explosion) with prior explanations. Based on similarities with other meteorite impact craters known at that time, the authors thought an impact origin was likely. Definitive proof of cosmic origin was uncovered in the 1970s after extensive drilling and trenching, and geophysical and geochemical studies, by the Geological Survey of India (GSI) [4].

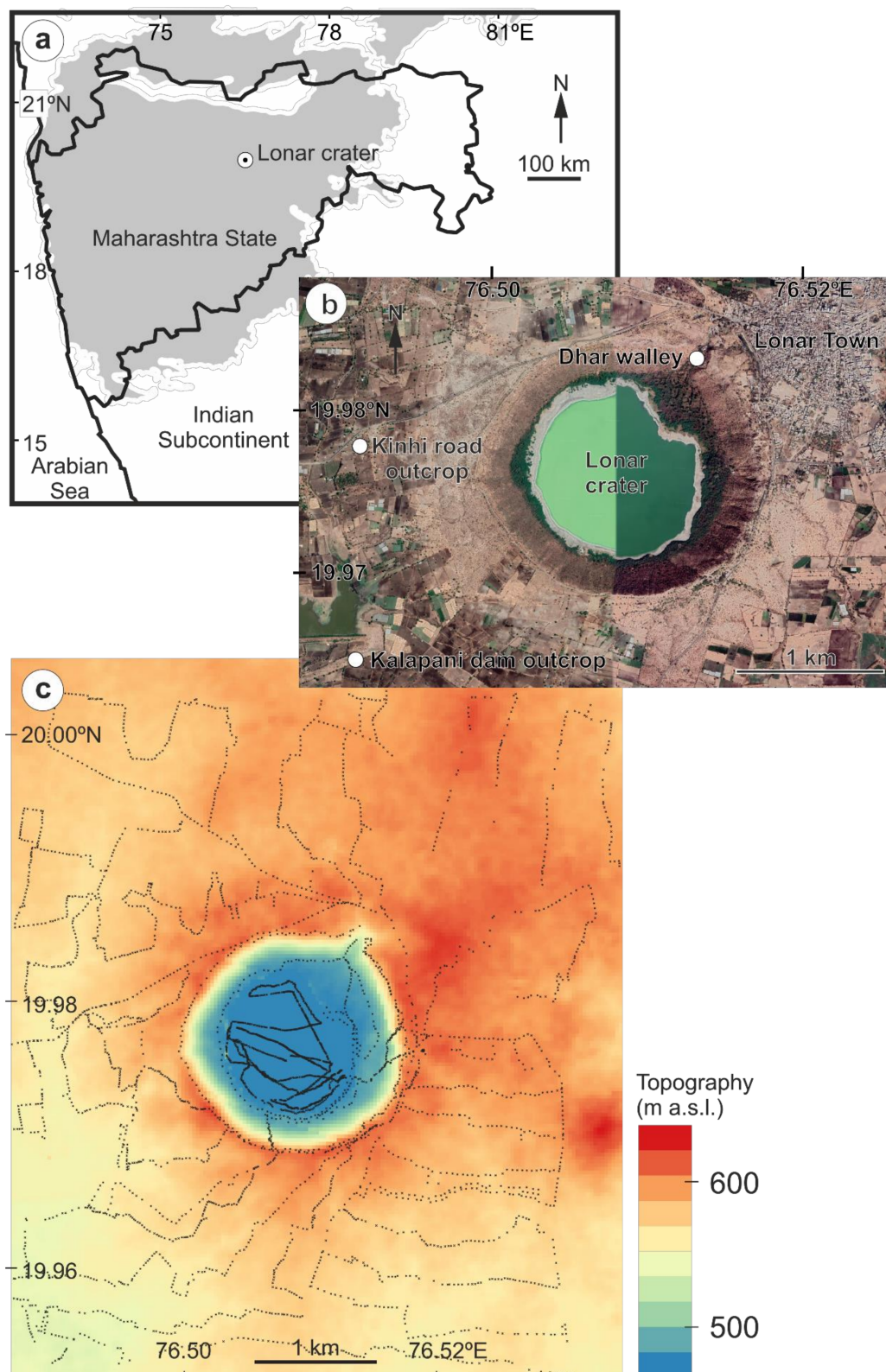


Figure 1. (a) Location of the Lonar meteorite impact crater in Maharashtra State, India. Grey indicates the distribution of Deccan Traps. The black line shows the border of Maharashtra state. (b) Composition of satellite images (Google) of the Lonar crater with sites mentioned in the text. (c) Topographic map as based on SRTM v3.0, <http://srtm.csi.cgiar.org>. The map includes locations of individual magnetic field measurements (black dots).

The Lonar impact crater has been formed into basaltic rocks, making it an analogy for lunar or Mars craters, and thus providing a fascinating source for meteorite impact studies. Three more craters that have been formed into basalts exist on Earth. These are the 20 km diameter Logancha crater in Russia [9], the 12 km diameter Vargeão Dome [10], and the 9.5 km diameter Vista Alegre crater in Brazil [11]. Among these, Lonar is easiest to access and most extensively studied so far.

The target of Lonar, the Deccan Traps (the Deccan large igneous province) is a vast extrusion (Figure 1a) of tholeiitic basaltic lava formed near the Cretaceous–Paleogene (K–Pg) boundary. Deccan volcanism took place over several million years from 69 to 62 Ma with periods of activity and inactivity [12,13], although the exact duration and age estimates are contested by different authors. Basaltic lavas covered an area of $1\text{--}2.6 \times 10^6 \text{ km}^2$ [14], of which $0.5 \times 10^6 \text{ km}^2$ now remains following erosion [15,16]. The maximum thickness of the traps is 1.8 to 2.4 km, and the traps are thicker in the west and thinner in the east [17,18]. In the Lonar area, the thickness of the Deccan Trap is thought to be between 400 and 700 m [19–21]. Inside the Lonar crater, at the inner slope of the rim, six outcroppings of 10 to 25 m thick fractured and tilted basalt flows are present. Characteristic red paleosol exists between flows due to weathering between consecutive flow extrusions [2].

The Lonar crater is a near circular depression with a depth of $\approx 135 \text{ m}$ (Figures 1b and 2). The elevation at the base of the inner rim wall is 475 m a.s.l. and the rim height is up to 600 m a.s.l., reaching 20–30 m over the surrounding flat plane (Figure 1c). The bedrock at the rim dips radially from the crater center at angles of $8\text{--}20^\circ$ with some patches of overturned bedrock and, characteristic for impact craters, stratigraphically inverted ejecta [2,4,19,22]. Because of ongoing erosion, the original crater could have had a rim crest diameter of 1.7–1.8 km with a rim height of about 40–70 m [2,19,22].

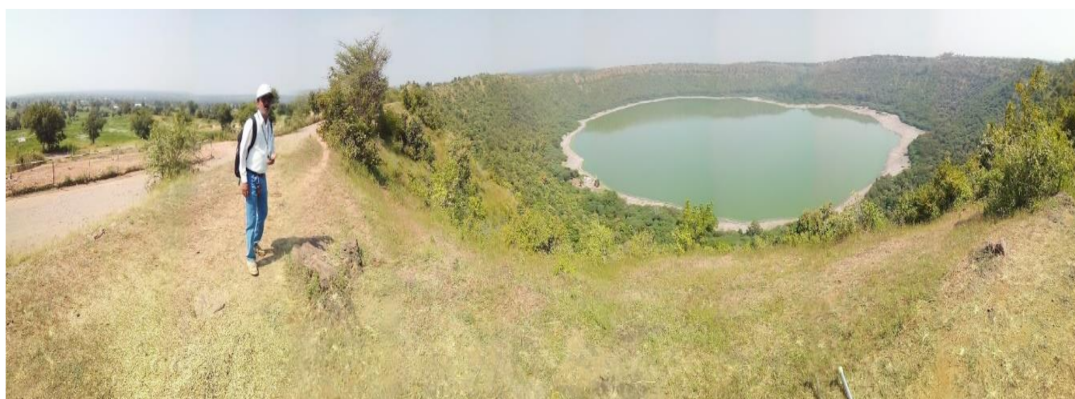


Figure 2. Panorama view of the Lonar crater from the south-eastern portion of the rim. The rim-to-rim diameter of the crater is 1.88 km and the vertical distance down to the lake is about 135 m. The maximum depth of the lake has fluctuated between 1.8 and 6.8 m since 1953 [23]. Photo by Jüri Plado.

A shallow alkaline lake with fluctuating water depth occupies the middle part of the crater depression (Figures 2 and 3). Water levels between 1.8 and 6.8 m have been recorded since 1953 (see an overview by [23]) depending on the amount of local rainfall. Dhar valley (Figure 3), which has a perennial stream, runs into the crater from the NE and has formed an alluvial fan that distorts the circularity of the lake. In addition to the Dhar valley, two perennial and one seasonal spring are also present [23].

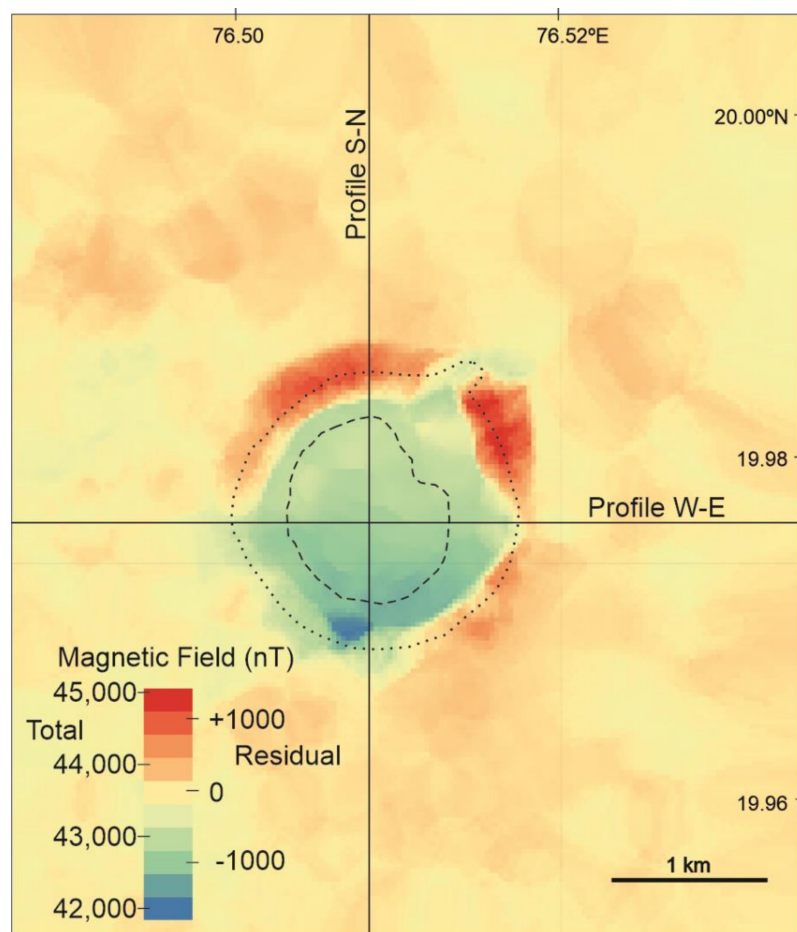


Figure 3. Total and residual magnetic field of the Lonar crater and its nearest surroundings. The dashed line represents the lake and the dotted line the crater rim. Coordinates are in WGS 84.

The Geological Survey of India drilled a profile of five 300 to 400 m deep (from the lake surface) holes at the Lonar Lake. Based on drilling results [7,24], a post-impact sediment lens with thickness of 60–100 m occurs under the lake. The sediment lens consists of silty clay with occasional glass and lithic fragments [19]. Below the sediments, the breccia lens occurs, which consists of alternating patches of coarse breccia (rock fragments of meters to tens of meters in size) and microbreccia/basalt powder (fragments of a few centimeters to submicroscopic in size). Coarse breccia fragments show low or no shock metamorphism, whereas microbreccia exhibits moderate to strong shock metamorphism [4]. The breccia lens is described [4] as disorganized: coarse breccia clasts are separated from each other by patches of microbreccia with a size of up to tens of meters. Initially, it was thought that all boreholes penetrated the breccia lens [4], but a later interpretation by [19] suggested that four of these did not reach the true bottom—the boundary between the underlying shocked target rocks and breccia. The deepest borehole bottomed in basaltic powder, but the definitive delineation of breccia and the true crater bottom was thought to be impossible to delineate even for this hole. Thus, the exact extent of the brecciated zone is unknown, but according to drilling data it is >225 m thick and limited to the bottom 500–600 m below the crater floor (unpublished work by S.S. Rao as cited in [2,25]). The volume of the lens is calculated to be about 0.23 km³ [26].

According to [2,19], ejecta surrounds the crater as an uninterrupted layer which spreads to an average distance of 2200 m from the center. Past this distance, the ejecta blanket is patchy. The ejecta layer shows little to no erosional features, thus, originally the continuous ejecta layer must have reached only slightly greater distances [19]. Reference [4] divided the ejecta into two types: (i) lower, poorly stratified clasts and blocks, which show no evidence of shock; and (ii) an upper, ≈1 m thick layer that

contains little to intensely shocked clasts, patches of impact glass, and spherules. The uppermost shocked ejecta blanket was found by [4] to extend ≈ 600 m continuously from the crater rim with shock pressure estimates for this ejecta reaching 60 GPa.

During a meteorite impact, several effects occur that can substantially alter the magnetic properties of rocks. These are impact, shock, temperature, and chemical [27,28]. The mechanical effect comes from the brecciation of the rock. Rock is broken into pieces and transported, and their original orientation becomes randomized. Due to this process, rock magnetic remanence directions are also oriented randomly, reducing the overall remanence intensity of the brecciated rocks.

Shock pressures of >1 GPa can reduce existing remanent magnetization and remagnetize rocks in the direction of the prevailing magnetic field at the time of impact [29], decrease magnetic susceptibility (MS) at >10 GPa [30], or produce new magnetic minerals at >40 GPa and >1000 °C [31]. Thermal effects prevail in the center of impact, where temperatures over the Curie temperatures of ferromagnetic minerals cause magnetic resetting. Within the simple Lonar impact crater, peak shock temperatures above the Curie temperature of iron oxides and high pressures are restricted to tiny amounts of rock in the central part only [32] and have been ineffective for most of the impactites. Post-impact chemical effects through hydrothermal alteration might create new magnetic mineral phases, e.g., oxidation of magnetite to hematite, and thus, reduction of magnetization [33].

Only one surface-based geomagnetic survey exists [25] that attempts to model the magnetic anomaly within the Lonar crater. Here, we aim to obtain a wider understanding of the magnetic anomaly caused by the impact. To achieve this, we performed ground-magnetic mapping of the Lonar crater and the nearby surroundings. A 2.5D magnetic model was produced from these measurements.

2. Previous Geophysical Research at the Lonar Crater

Gravity, magnetic, and seismic investigations were carried out at the Lonar crater in February 1964 by the GSI [34]. This unpublished report is, unfortunately, inaccessible to the wider public, but results were found to be described in a report by [24]. Further gravity work was conducted in November 1977 [19]. Based on those potential field data, in addition to [35] and [36], a geophysical model of the crater interior was produced by [25].

Gravity measurements made in 1964 [34] indicated the presence of a negative anomaly. The results were incorporated into a gravity study by [19], who observed an anomaly of ≈ 3.6 mGal in amplitude, with a negative part of -2.25 mGal at the crater center and a positive part of about $+1.4$ mGal at the rim. The anomaly was found to be circular, but the interpreted isolines were slightly elliptical in the very central part with a longer axis oriented NW–SE.

Total magnetic intensity (TMI) measurements were made outside the crater structure along eight radial lines and within the crater along seven north–south-oriented traverses [34]. Magnetic anomalies of a few thousands of nT in amplitude were stated to positively correlate with the topography. Over the crater lake a uniform regular increase (≈ 1000 nT/km) of the magnetic field was discovered and attributed to (i) sub-trap topography and (ii) remanent magnetization of the trap. Ref. [25] described a vertical component magnetic anomaly of 550 nT in amplitude over the crater floor. Their data were taken from magnetic field vertical component measurements by [35]. Their profile shows anomalous values of -30 nT at the shoreline on the SW side of the Lonar lake, but values increase toward the center of the lake until a maximum of $+340$ nT at the crater center. Then, toward NE, the values decrease rapidly back to zero.

Seismic sounding was conducted in the lake and at the lakeside within the crater [34]. Two distinct layers were seen overlying the hard trap. According to seismic studies, the bottom hard trap floor varies from 91 m at the NE to 183 m at the lake center. With data from shot points not completely available, drawing seismic profiling across the crater was deemed impossible and the bedrock position was not determined.

Several studies [25,32,37–41] are dedicated to rock magnetic properties of Lonar with varying results leading to differing interpretations. Two components of remanent magnetization have been

found, i.e., (i) low coercivity-low temperature (LC/LT) and (ii) high coercivity-high temperature (HC/HT) components. The LC/LT component is orientated towards the present Earth magnetic field and is of chemical (CRM) or viscous (VRM) origin. Shock remanent magnetization (SRM) of this component was argued by [39] only. Some studies [32,38,41] claim that the SRM was either not acquired or is overwritten by the VRM and/or CRM. The HC/HT component in basalts is carried by a single-domain titanomagnetite [42]. It is argued by [38] and [41] that the HC/HT component was altered by the impact. Refs. [32,37] suggest the opposite, showing pressures to be too low for any change to occur (0.2–0.5 GPa by [37] and <1 GPa by [32]).

3. Materials and Methods

A total of 203 in situ MS measurements with magnetic susceptibility meter SM-30 (ZH Instruments) were carried out on lake sediments, outcropping inner wall basalts, and ejecta (the road to the Kinhi and Kalapani dam outcrops; Figure 1b). These data were used to adjust the magnetic model.

Ground magnetic measurements were carried out in October 2017 using two proton precession magnetometers G-856 (Geometrics). The land survey was conducted along variously oriented tracks by taking readings at approximately every 35 m. A rubber rowing boat was used to host magnetometer and operators during the measurements at the lake. In total, an area of 36 km² was covered (Figure 1c). Measurements made during the period of nine days were corrected against diurnal variations. For correction, a control point was established where the magnetic field strength was measured at the beginning and end of individual runs. The control data were used to level the closest magnetic observatory data (by World Data Centre for Geomagnetism, Mumbai; 18°53'36" N, 72°48'54" E), which were applied. The amplitude of diurnal variations was up to 50 nT, which is a minor change compared to the total amplitude of the magnetic field by the crater structure. Individual measurement data were interpolated in QGIS v.3.2.3 using the SAGA toolkits Universal kriging algorithm (cell size = 30).

Software Potent v4.16.07 by Geophysical Software Solutions was used in the forward modelling of the Lonar crater anomaly. The inducing field parameters were estimated from the International Geomagnetic Reference Field (IGRF): field intensity $F = 43,722$ nT, declination $D = -0.2^\circ$, and inclination $I = 29.3^\circ$. Potent allows an interactive 2.5-dimensional-representation of subsurface model volumes with a polygonal cross-section and variable strike length. Our model consists of polygonal prisms for which we calculated a magnetic response curve with two profiles, (i) south–north- and (ii) west–east-oriented, that crossed the center of Lonar crater (Figure 3). By changing the shapes of prisms, we matched the model-produced curves to fit the observed data by trial-and-error techniques. Because of the number of several independent variables (magnetic susceptibility, intensity, the direction of remanent magnetization, and shape of the polygons), and the inverse problem of potential field interpretation, the model is not unique. Topographic data (Figure 1c) are based on SRTM v3.0 (<http://srtm.csi.cgiar.org>).

Magnetic anomaly modelling software, such as Potent, allows only MS to be set as a background magnetic property. This is adequate for studies of ore bodies, which usually have higher magnetization compared to the host. It is, however, inadequate in the case of the Lonar crater, where background basalts, in addition to their high magnetic susceptibility, have high remanent magnetization (Table 1). Furthermore, the remanence directions (Table 2) are different from the direction of the present-day Earth magnetic field. For this reason, first, the Deccan Trap was modelled as a large background body hosting the Lonar magnetic anomaly model.

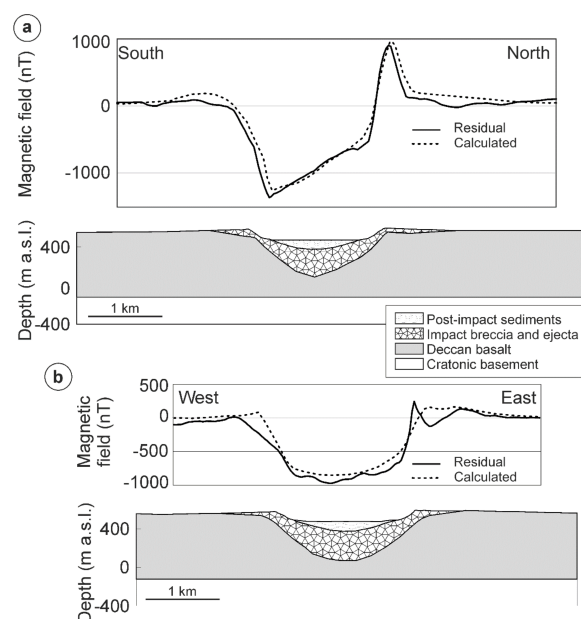
Table 1. Magnetic susceptibility of Deccan Trap basalts and Lonar crater rocks/sediments according to earlier research and the present study [37,39,43,44].

	Magnetic Susceptibility (10 ⁻⁶ SI)				Q-Ratio (-)
	Average	Min.	Max.	St.dev.	
Deccan Traps					
Lonar lake [39]	26,000	17,000	40,200	7200	2.5–10.1
Saurashtra [44]	55,000				Average 5.93
Dhar region [43]	43,800	15,700	72,000		1
Lonar lake [37]	39,500	26,000	55,800	15,200	2.35–9.81
Present study					
Lonar basalts (n = 89)	24,000	11,200	65,500	9532	
Lonar lake silt sediments (n = 46)	3100	700	7900	2100	
Lonar lake basalt sand (n = 5)	13,580	10,900	21,400	3900	
Lonar paleosols (n = 5)	6100	4930	9330	2470	
Road to Kinhi outcrop					
ejecta (n = 16)	7900	3560	11,400	2141	
basalt boulders (n = 1)			24,400		
Kalapani dam outcrop					
ejecta (n = 27)	7000	2390	8820	1425	
basalt boulders (n = 14)	19,400	12,400	30,500	4970	

Table 2. Parameters of the bodies used in modelling.

Body	Magnetic Susceptibility (10^{-6} SI)	Natural Remanent Magnetization			Q-Ratio (-)	Side Length (m)	Density (g/cm^3)
		Intensity (A/m)	Declination ($^{\circ}$)	Inclination ($^{\circ}$)			
Post-impact sediments	6000	0.21	0	10	1.0	1100	2.07
Breccia lens	24,000	0.0	n.a.	n.a.	1.0	1850	2.60
Deccan Trap	40,000	4.2	150	48	3.0	100,000; ∞	2.72

As a result of the modelling (Figure 4a,b), a close match to the observed anomaly is obtained. Figure 4a shows the magnetic anomaly profile in the S–N direction and Figure 4b the W–E cross-section. The cross-section line in the software is drawn with an assigned width of 30 m, which matches the cell size of the magnetic field interpolation. The final results were smoothed against irregularities.

**Figure 4.** Residual and calculated magnetic profiles and models trending (a) S–N and (b) W–E (see Figure 3 for location).

4. Results

4.1. Magnetic Field

On a large scale, the magnetic anomaly (Figure 3) of the Lonar impact crater coincides with the topography (Figure 1c). Distinct are the rim and crater depression. All of the crater depression is characterized by a negative residual magnetic field. Relative to the zero level (corresponding to the regional field value of 43,637 nT), the residual magnetic field map (Figure 3) depicts a circular negative anomaly of about −1000 nT on average. The negative field within the depression is, however, not uniform because values are increasing while moving from south (about −1200 nT) to north (about −600 nT) with a gradient of about 1000 nT/km. The gradient is similar to that measured across the lake by [34].

The rim is associated with high anomalous crescent-shaped positive values in north-western (up to +1250 nT) and north-eastern (up to +1400 nT) segments. These two positive anomalies are separated by a negative incision (down to −900 nT) that coincides with the Dhar valley. Although the south-eastern rim is still characterized by positive values (up to +900 nT), the southern and south-western sections are negative (down to −700 nT) or zero anomalies. In a radial direction, the width of the rim anomalies is about 250–350 m. As described below, the lack of Deccan magnetic masses and direction of magnetization are responsible for the rim anomalies, rather than the rim feature of the Lonar impact crater.

The magnetic field beyond the crater changes chaotically with amplitudes locally up to 1000 nT. The width of these anomalies is less than 500 m, and often less than 200 m, indicating their relatively shallow sources are related to heterogeneities in magnetic properties within the Deccan Trap basalts and/or relationship to the thickness of overburden and weathering. In the area under discussion, no deep-source regional feature exists, e.g., significant undulation of sub-trap topography, that could mask the magnetic signatures associating with the Lonar structure.

4.2. Magnetic Properties

Deccan basalts, a target for the Lonar-forming projectile, are highly magnetic, which is illustrated by high values of both induced and remanent magnetizations (Table 1). Our in situ measurements of the MS are well comparable with earlier studies by [37,39,43,44]. By our data, measured from outcrops at the inner slope of the crater, the Deccan basalts have an average MS value of $24,000 \times 10^{-6}$ SI. Weathered basalts, i.e., paleosols occurring between individual basalt flows, exhibit an average value of 6110×10^{-6} SI. High remanent magnetization of Deccan basalts is illustrated by Koenigsberger ratios that, based on the literature (Table 1), are between 1 and 10.1.

Lake sediments consist of grey, brown, or black silt, and black basaltic sand. The silt of different colors constitutes a topmost layer, under which black sand was sometimes reached. Silt sediments have average k values of 3100×10^{-6} SI. The black basaltic sand has a variable MS between 10,000 and $21,000 \times 10^{-6}$ SI.

Ejecta at Kinhi and Kalapani Dam (Figure 1b) has average MS values of 7900×10^{-6} SI and 7000×10^{-6} SI, respectively. These values are similar to those measured in the matrix of paleosols. Basalt boulders within the ejecta exhibit values similar to the basalts in the crater inner wall: $24,400 \times 10^{-6}$ SI in Kinhi and $19,414 \times 10^{-6}$ SI in Kalapani Dam outcrops.

4.3. Model

A geological model (Figure 4) was constructed of three 2.5D polygonal prisms. From top to bottom, the bodies represent (i) post-impact sediments, (ii) lens of allochthonous breccia and ejecta, and (iii) Deccan Trap basalts. Strike length (Table 2) of prisms is variable but comparable to the length of prisms along with the profile. Side space of (i) and (ii) was filled with prisms that have magnetic properties of (iii).

The magnetic susceptibility value of 6000×10^{-6} SI was assigned to the post-impact sediments, $24,000 \times 10^{-6}$ SI for the allochthonous breccia/ejecta, and $40,000 \times 10^{-6}$ SI to the Deccan Trap basalts (Table 2). We assumed remanent magnetization of post-impact sediments is equal to induced magnetization ($Q = 1$) and is roughly directed toward the present magnetic field. Magnetic susceptibility data for breccia in drill cores at the lake are unavailable, so we used values that were measured from fractured basalts at the inner rim and basaltic boulder within ejecta as best analogues available. The NRM characteristics of breccia are assumingly low on a large scale. During brecciation, the pieces of rock are moved and oriented randomly, as are their original remanence directions, negating the NRM. Thus, no remanent magnetization was applied to breccia and ejecta.

Deccan Trap basalts have the greatest amount of published data available on their magnetic properties. The average of published values, $40,000 \times 10^{-6}$ SI, was chosen to represent basalts (Table 2). Natural remanent magnetization intensity averages are between 4.1–4.8 A/m [32,39,42]. A value of 4.2 A/m was chosen, making Q equal to 3. Declination and inclination measured at Deccan basalts range from 110 to 165° and 44 to 61°, respectively [32,45,46]. Values of 150° (declination) and 48° (inclination) fit the model best.

The modelled polygonal prisms were shaped by topographic [SRTM v3.0, <http://srtm.csi.cgiar.org>] and GSI drill hole data [4,24]. As a base for the model, results of a numerical simulation of the impact by [32] were used. A prism for post-impact sediments, with a strike length of 1100 m, was constructed as a lens with a maximum thickness at the crater center (100 m). Underneath was a lens of breccia with a side length of 1850 m and central thickness of 260 m. Third, the lowermost prism was used to simulate the Deccan Traps. It was a rectangle-shaped body with an infinite side length, extending to a depth of 700 m [19].

On the south–north-trending profile (Figure 4a) a distinct negative anomaly of the crater floor and the positive anomaly of the N–NW rim are observed. The vast amount of the magnetic field anomaly is produced by the highly magnetized Deccan Trap basalts with their high MS and strong SE-directed remanent magnetization (Table 2). Thus, the strong positive anomalies seen at the northern rim, and the negative near the southern rim were due to strong remanent magnetization of Deccan basalts and the topographic effect of the Lonar crater.

Profile 2 (Figure 4b) is W–E trending. A bowl-shaped anomaly is observed with negative values down to -1000 nT at the crater center. Negative values decrease toward the rim of the crater, remaining slightly negative at the west and close to zero at the east. At the eastern rim exists a combination of negative and positive relatively short wavelength (half width <200 m) anomalies of 250 nT in amplitude. These anomalies, like many others in the surroundings of Lonar, are likely due to magnetic heterogeneities within the basaltic target.

5. Discussion

Compared to the basalt-produced anomaly, the magnetic effect due to a combination of impact breccias, ejecta, and post-impact sediments is weak with an amplitude of less than 150 nT. The present model is composed on our best knowledge [2,19,24,32,34] of the inner structure of Lonar. Changing the shape and physical parameters of impact-related lithologies has a minor influence on the calculated field, compared to the overwhelming effect by basaltic target.

Thus, the majority of the magnetic field in Lonar is due to topographic effects, which are pronounced by high magnetization of target basalts. Topographic effects on magnetic data have been talked about as early as the 1970s regarding ocean floor measurements [47]. By nature, an anomaly appears when a magnetic intensity or susceptibility contrast exists. This is caused by a difference between rock formations or a topographical feature such as a deep valley facilitating a rock–air contrast. The additional effect occurs due to inclined magnetic field interaction with slopes [48]. The Lonar crater has been formed into the Deccan Traps, which have high induced magnetization and even stronger remanent magnetization intensity. In contrast to basalts, the post-impact sediments, breccia, and air, which in combination fill the true crater, are magnetized to a much lesser degree. For this reason,

the Deccan traps generate most of the residual field of the crater and the estimation of the true crater configuration is paramount in describing the magnetic anomaly of the breccia/post-impact sediments.

The estimation of negative and positive landform topographical effects on magnetic data is important. Left unaccounted for, interpretations may be geologically erroneous and might obscure the magnetic signal for geological bodies of interest. This is demonstrated for positive landforms by [49] and negative landforms by [48]. If the topographical effect was not assessed in the case of the Lonar crater, interpretation of the residual field would require a highly magnetized body to exist under the lake.

Similar to [34], we note a regular increase (≈ 1000 nT/km) of the magnetic field within the depression. Different from the interpretation of these authors, our model indicates that this change is produced purely by the magnetization direction of the trap and is not related to potentially undulating sub-trap topography.

A geological model of the crater interior, based on earlier vertical component magnetic and gravity data, was proposed by [25]. Their model was based on vertical component measurements over the lake only, and showed a positive anomaly at the crater center with magnetic lows toward the SW and NE. To account for this positive anomaly, they modelled high susceptibility ($14,000 \times 10^{-6}$ SI and $40,000 \times 10^{-6}$ SI) dike-like bodies within the 5000×10^{-6} SI breccia and interpreted them as having high magnetization due to concentration of magnetite that may represent fragments of the meteorite. In stark contrast, our study shows a low-gradient negative total vector anomaly in the crater depression with no need for a high magnetic susceptibility body to explain the observed magnetic anomaly. Our magnetic data suggest that the breccia is rather uniformly magnetized. Due to brecciation and random distribution of clasts and their remanent magnetizations, the net remanent magnetization is significantly weaker or nonexistent compared to the surrounding Deccan Traps. In addition, we note that the meteorite impact process, as described, e.g., by [50] and many others, does not favor the concentration of meteoritic matter within certain regions of allochthonous breccia. Moreover, based on Co, Cr, and Ni enrichment in impact spherules, and because no Fe-Ni fragments, phases, nor other impactor fragments have been found, the impactor of Lonar is thought [51,52] to be a chondrite, type of meteorite that is depleted by all siderophile elements.

Previous gravity measurements [19,34] have shown typical to simple craters (e.g., Granby and Tvären in Sweden [53]), i.e., a bowl-shaped negative anomaly. The maximum amplitude of the anomaly is -3.6 mGal, which is relatively strong for a 1.88 km-sized crater structure (see [33,54]). The amplitude is likely amplified by the presence of water and low-density post-impact sediments.

Initially, it was thought the drilling of the breccia lens in the 1970s penetrated it [4] but that idea was rejected by [19]. The deepest drill-hole reached 400 m and bottomed in basaltic powder. The nature of the breccia is quite complicated with large blocks of breccia, meters in size, separated by meters of powder. The model created here reaches deeper (500 m for breccia bottom) than the drill holes at Lonar. Refs. [25] and [26] also suggested the depth to the true crater to be greater, 500 and 460 m, respectively. Likely, the true bottom of the crater has not been penetrated by drillings.

6. Conclusions

The Lonar meteorite impact crater is well seen in magnetic field data in the background of a smooth regional field. The crater produces a negative magnetic anomaly ranging from about -1200 nT to -600 nT in the southern and northern parts of the crater depression, respectively. Most of the rim is characterized by positive anomalies of up to $+1400$ nT. The southern and southwestern sections of the rim show, however, negative anomalies down to -700 nT. The majority of the anomaly pattern is due to a topographic effect and strong SE directed natural remanent magnetization of Deccan Trap basalts. The total magnetic signal of the impact-produced allochthonous breccias and post-impact sediments is small, measuring less than 150 nT. Unlike an earlier study by [25], no short-wavelength magnetic anomalies, which could correspond to concentrations of magnetic material within allochthonous breccias, were found.

Author Contributions: Conceptualization, J.P., M.L. and K.K.; methodology, J.P., K.K. and M.L.; software, K.K. and J.P.; validation, K.K. and J.P.; formal analysis, K.K. and J.P.; investigation, K.K., J.P., M.L., S.H.J. and M.S.; resources, M.L., S.H.J.; data curation, K.K.; writing—original draft preparation, K.K. and J.P.; writing—review and editing, K.K. and J.P.; visualization, J.P. and K.K.; supervision, J.P.; project administration, K.K.; funding acquisition, J.P. All authors have read and agreed to the published version of the manuscript.

Funding: Work by J.P. was supported by the Estonian Research Council (IUT20-34).

Acknowledgments: We acknowledge the Erasmus+ programme by the European Commission for providing support for scientific exchange. Sharat Raj B. from the Central University of Karnataka, India, is acknowledged for help during fieldwork. We are thankful to two anonymous reviewers for the revision of the paper.

Conflicts of Interest: The authors declare no conflict of interest. The funders had no role in the design of the study; in the collection, analyses, or interpretation of data; in the writing of the manuscript, or in the decision to publish the results.

References

1. Sengupta, D.; Bhandari, N. Formation age of the Lonar Crater. *Abstr. Pap. Submitt. Lunar Planet. Sci. Conf.* **1988**, *19*, 1059–1060.
2. Maloof, A.C.; Stewart, S.T.; Weiss, B.P.; Soule, S.A.; Swanson-Hysell, N.L.; Louzada, K.L.; Garrick-Bethell, I.; Poussart, P.M. Geology of Lonar Crater, India. *Geol. Soc. Am. Bull.* **2010**, *122*, 109–126. [\[CrossRef\]](#)
3. Jourdan, F.; Moynier, F.; Koeberl, C.; Eroglu, S. ⁴⁰Ar/³⁹Ar age of the Lonar crater and consequence for the geochronology of planetary impacts. *Geology* **2011**, *39*, 671–674. [\[CrossRef\]](#)
4. Fredriksson, K.; Dube, A.; Milton, D.J.; Balasundaram, M.S. Lonar Lake, India: An Impact Crater in Basalt. *Science* **1973**, *180*, 862–864. [\[CrossRef\]](#)
5. Gilbert, G.K. The origin of hypotheses illustrated by the discussion of a topographic problem. *Science* **1896**, *3*, 1–13. [\[CrossRef\]](#)
6. Cotton, C.A. *Volcanoes: As Landscape Forms*; Whitcombe and Tombs Ltd.: Christchurch, New Zealand, 1952.
7. Nandy, N.; Deo, V. Origin of the Lonar Lake and its alkalinity. *TISCO* **1961**, *8*, 144–155.
8. Lafond, E.C.; Dietz, R.S. Lonar Crater, India, a Meteorite Crater? *Meteoritics* **1964**, *2*, 111–116. [\[CrossRef\]](#)
9. Masaitis, V.L. Impact structures of northeastern Eurasia: The territories of Russia and adjacent countries. *Meteorit. Planet. Sci.* **1999**, *34*, 691–711. [\[CrossRef\]](#)
10. Crosta, A.P.; Kazzuo-Vieira, C.; Pitarello, L.; Koeberl, C.; Kenkmann, T. Geology and impact features of Vargeão Dome, southern Brazil. *Meteorit. Planet. Sci.* **2012**, *47*, 51–71. [\[CrossRef\]](#)
11. Crosta, A.P.; Vasconcelos, M.A.R. Update on the current knowledge of the Brazilian impact craters. *Lunar Planet. Sci. Conf.* **2013**, *44*, 4–5.
12. Chenet, A.; Quidelleur, X.; Fluteau, F.; Courtillot, V.; Bajpai, S. ⁴⁰K–⁴⁰Ar dating of the Main Deccan large igneous province: Further evidence of KTB age and short duration. *Earth Planet. Sci. Lett.* **2007**, *263*, 1–15. [\[CrossRef\]](#)
13. Pande, K. Age and duration of the Deccan Traps, India: A review of radiometric and paleomagnetic constraints. *J. Earth Syst. Sci.* **2002**, *111*, 115. [\[CrossRef\]](#)
14. Vaidhyanathan, R.; Ramakrishnan, M. *Geology of India*; Geological Society of India: Bangalore, India, 2008; Volume 2, pp. 733–784.
15. Philpotts, A.; Ague, J. *Principles of Igneous and Metamorphic Petrology*; Cambridge University Press: Cambridge, UK, 2009. [\[CrossRef\]](#)
16. Jay, A.E.; Widdowson, M. Stratigraphy, structure and volcanology of the SE Deccan continental flood basalt province: Implications for eruptive extent and volumes. *J. Geol. Soc.* **2008**, *165*, 177–188. [\[CrossRef\]](#)
17. Chenet, A.L.; Courtillot, V.; Fluteau, F.; Gérard, M.; Quidelleur, X.; Khadri, S.F.R.; Subbarao, K.V.; Thordarson, T. Determination of rapid Deccan eruptions across the Cretaceous-Tertiary boundary using paleomagnetic secular variation: 2. Constraints from analysis of eight new sections and synthesis for a 3500-m-thick composite section. *J. Geophys. Res.* **2009**, *114*, 6103. [\[CrossRef\]](#)
18. Harinarayana, T.; Patro, B.P.K.; Veeraswamy, K.; Manoj, C.; Naganjaneyulu, K.; Murthy, D.N.; Virupakshi, G. Regional geoelectric structure beneath Deccan Volcanic Province of the Indian subcontinent using magnetotellurics. *Tectonophysics* **2007**, *445*, 66–80. [\[CrossRef\]](#)
19. Fudali, R.F.; Milton, D.J.; Fredriksson, K.; Dube, A. Morphology of Lonar Crater, India: Comparisons and implications. *Moon Planets* **1980**, *23*, 493–515. [\[CrossRef\]](#)

20. Subbarao, K.V.; Chandrasekharam, D.; Navaneethakrishnan, P.; Hooper, P.R. *Stratigraphy and Structure of Parts of the Central Deccan Basalt Province: Eruptive Models*; Volcanism, Wiley Eastern Ltd.: New Delhi, India, 1994; pp. 321–332.
21. Subbarao, K.V. *Deccan Volcanic Province: Memoir 43 (1 and 2)*; Geological Society of India: Bangalore, India, 1999.
22. Nakamura, A.; Yokoyama, Y.; Sekine, Y.; Goto, K.; Komatsu, G.; Kumar, P.S.; Matsuzaki, H.; Kaneoka, I.; Matsui, T. Formation and geomorphologic history of the Lonar impact crater deduced from in situ cosmogenic ¹⁰Be and ²⁶Al. *Geochem. Geophys. Geosyst.* **2014**, *15*, 3190–3197. [[CrossRef](#)]
23. Reddy, D.V.; Madhav, T.; Chandrakala, P.; Nagabhushanam, P. A perspective of alkaline Lonar Lake, Maharashtra, India with reference to its hydrochemistry. *Curr. Sci.* **2015**, *109*, 965–975. [[CrossRef](#)]
24. Dube, A.; Gupta, S. *Detailed Investigation of Lonar Crater Buldana District, Maharashtra*; Geological Survey of India: Bangalore, India, 1980.
25. Rajasekhar, R.P.; Mishra, D. Analysis of gravity and magnetic anomalies over Lonar lake, India: An impact crater in a basalt province. *Curr. Sci.* **2005**, *88*, 1836–1840.
26. Grieve, R.A.F.; Garvin, J.B.; Coderre, J.M.; Rupert, J. Test of a geometric model for the modification stage of simple impact crater development. *Meteoritics* **1989**, *24*, 83–88. [[CrossRef](#)]
27. Pohl, J.; Bleil, U.; Hornemann, U. Shock magnetization and demagnetization of basalt by transient stress up to 10kbar. *J. Geophys.* **1975**, *41*, 23–41.
28. Gilder, S.A.; Pohl, J.; Eitel, M. *Magnetic fields in the Solar System*; Lühr, H., Wicht, J., Gilder, S., Holschneider, M., Eds.; Springer: Dordrecht, The Netherlands, 2018; Chapter 13; pp. 357–382.
29. Hargraves, R.B.; Perkins, W.E. Investigations of the effect of shock on natural remanent magnetism. *J. Geophys. Res.* **1969**, *74*, 2576–2589. [[CrossRef](#)]
30. Reznik, B.; Kontny, A.; Fritz, J. Effect of moderate shock waves on magnetic susceptibility and microstructure of a magnetite-bearing ore. *Meteorit. Planet. Sci.* **2017**, *52*, 1495–1504. [[CrossRef](#)]
31. Chao, E.C.T. *Pressure and Temperature Histories of Impact Metamorphosed Rocks—Based on Petrographic Observations*; Mono Press: Baltimore, MD, USA, 1968; pp. 135–158.
32. Louzada, K.L.; Weiss, B.P.; Maloof, A.C.; Stewart, S.T.; Swanson-Hysell, N.L.; Soule, S.A. Paleomagnetism of Lonar impact crater, India. *Earth Planet. Sci. Lett.* **2008**, *275*, 308–319. [[CrossRef](#)]
33. Pilkington, M.; Grieve, R.A.F. The geophysical signature of terrestrial impact craters. *Rev. Geophys.* **1992**, *30*, 161. [[CrossRef](#)]
34. Kailasam, L.N.; Gupta Sarma, D.; Bhanumurth, Y.R.; Das, P.C. *Research Report*; Geological Survey of India: Kolkata, India, 1964; Unpublished.
35. Subrahmanyam, B. Lonar Crater, India: A Crypto-Volcanic Origin. *Geol. Soc. India* **1985**, *26*, 326–335.
36. Fudali, R.F.; Subrahmanyam, B. Gravity reconnaissance at Lonar Crater, Maharastra. *Spec. Publ. Ser. Geol. Surv. India* **1983**, *2*, 83–87.
37. Agarwal, A.; Kontny, A.; Srivastava, D.C.; Greiling, R.O. Shock pressure estimates in target basalts of a pristine crater: A case study in the Lonar crater, India. *Geol. Soc. Am. Bull.* **2015**, *128*, 19–28. [[CrossRef](#)]
38. Arif, M.; Basavaiah, N.; Misra, S.; Deenadayalan, K. Variations in magnetic properties of target basalts with the direction of asteroid impact: Example from Lonar crater, India. *Meteorit. Planet. Sci.* **2012**, *47*, 1305–1323. [[CrossRef](#)]
39. Rao, G.V.S.P.; Bhalla, M.S. Lonar Lake: Palaeomagnetic evidence of shock origin. *Geophys. J. Int.* **1984**, *77*, 847–862. [[CrossRef](#)]
40. Sangode, S.J.; Sharma, R.; Mahajan, R.; Basavaiah, N.; Srivastava, P.; Gudadhe, S.S.; Meshram, D.C.; Venkateshwarulu, M. Anisotropy of magnetic susceptibility and rock magnetic applications in the Deccan volcanic province based on some case studies. *J. Geol. Soc. India* **2017**, *89*, 631–642. [[CrossRef](#)]
41. Misra, S.; Arif, M.; Basavaiah, N.; Srivastava, P.K.; Dube, A. Structural and anisotropy of magnetic susceptibility (AMS) evidence for oblique impact on terrestrial basalt flows: Lonar crater, India. *Geol. Soc. Am. Bull.* **2010**, *122*, 563–574. [[CrossRef](#)]
42. Cisowski, S.M.; Fuller, M. The effect of shock on the magnetism of terrestrial rocks. *J. Geophys. Res. Solid Earth* **1978**, *83*, 3441–3458. [[CrossRef](#)]
43. Poornachandra Rao, G.V.S.; Bhalla, M.S. Palaeomagnetism of Dhar traps and drift of the subcontinent during the Deccan volcanism. *Geophys. J. Int.* **1981**, *65*, 155–164. [[CrossRef](#)]

44. Chandrasekhar, D.V.; Mishra, D.C.; Poornachandra Rao, G.V.S.; Mallikharjuna Rao, J. Gravity and magnetic signatures of volcanic plugs related to Deccan volcanism in Saurashtra, India and their physical and geochemical properties. *Earth Planet. Sci. Lett.* **2002**, *201*, 277–292. [\[CrossRef\]](#)
45. Vandamme, D.; Courtillot, V.; Besse, J.; Montigny, R. Paleomagnetism and age determinations of the Deccan Traps (India): Results of a Nagpur-Bombay Traverse and review of earlier work. *Rev. Geophys.* **1991**, *29*, 159. [\[CrossRef\]](#)
46. Athavale, R.N.; Anjaneyulu, G.R. Palaeomagnetic results on the Deccan trap lavas of the Aurangabad region and their tectonic significance. *Tectonophysics* **1972**, *14*, 87–103. [\[CrossRef\]](#)
47. Parker, R.L.; Huestis, S.P. The inversion of magnetic anomalies in the presence of topography. *J. Geophys. Res.* **1974**, *79*, 1587–1593. [\[CrossRef\]](#)
48. Ugalde, H.; Morris, B. An assessment of topographic effects on airborne and ground magnetic data. *Lead. Edge* **2008**, *27*, 76–79. [\[CrossRef\]](#)
49. Smekalova, T.N.; Bevan, B.W. The Magnetic Anomaly of a Mound; 2002. Available online: https://www.researchgate.net/publication/272489033_The_Magnetic_Anomaly_of_a_Mound (accessed on 20 October 2020).
50. Melosh, H.J. *Impact Cratering. A Geologic Process*; Oxford Monographs on Geology and Geophysics Series; Clarendon Press: Oxford, UK, 1989; ISBN 0 19 504284 0.
51. Das Gupta, R.; Banerjee, A.; Goderis, S.; Claeys, P.; Vanhaecke, F.; Chakrabarti, R. Evidence for a chondritic impactor, evaporation-condensation effects and melting of the Precambrian basement beneath the ‘target’ Deccan basalts at Lonar crater, India. *Geochim. Cosmochim. Acta* **2017**, *215*, 51–75. [\[CrossRef\]](#)
52. Misra, S.; Newsom, H.E.; Prasad, M.S.; Geissman, J.W.; Dube, A.; Sengupta, D. Geochemical identification of impactor for Lonar crater, India. *Meteorit. Planet. Sci.* **2009**, *44*, 1001–1018. [\[CrossRef\]](#)
53. Henkel, H.; Eknelligoda, T.C.; Aaro, S. The extent of impact induced fracturing from gravity modeling of the Granby and Tvären simple craters. *Tectonophysics* **2010**, *485*, 290–305. [\[CrossRef\]](#)
54. Plado, J.; Pesonen, L.J.; Puura, V. Effect of erosion on gravity and magnetic signatures of complex impact structures: Geophysical modeling and applications. In *Large Meteorite Impacts and Planetary Evolution II*; Dressler, B.O., Sharpton, V.L., Eds.; Geological Society of America Special Papers; Geological Society of America: Boulder, CO, USA, 1999; Volume 339, pp. 229–239. [\[CrossRef\]](#)

Publisher’s Note: MDPI stays neutral with regard to jurisdictional claims in published maps and institutional affiliations.



© 2020 by the authors. Licensee MDPI, Basel, Switzerland. This article is an open access article distributed under the terms and conditions of the Creative Commons Attribution (CC BY) license (<http://creativecommons.org/licenses/by/4.0/>).